The bigger picture: global analysis of solubilization performance of classical detergents versus new synthetic polymers utilizing shotgun proteomics

Stefan Mueller[a]*, Jan Kubicek[b], Felipe Merino[b], Philipp Hanisch[b], Barbara Maertens[b] and Jan-Wilm Lackmann[c]

[a]CECAD/ CMMC Proteomics Facility, Center for Molecular Medicine Cologne (CMMC) Universitaet Koeln, Robert-Koch-Str. 21, 50931 Köln, Germany

[b]Cube Biotech GmbH, Creative Campus Allee 12, 40789 Monheim, Germany

[c]CECAD/ CMMC Proteomics Facility, CECAD - Cluster of Excellence, Universitaet Koeln, Robert-Koch-Str. 21, 50931 Köln, Germany

*Correspondence to: stefan.mueller@uni-koeln.de

Abstract

Integral membrane proteins are critical for many cellular functions. Roughly 25% of all human genes code for membrane proteins, and about 70% of all approved drugs target them. Despite their importance, laborious and harsh purification conditions often hinder their characterization. Traditionally, they are removed from the membrane using detergents, thereby taking the proteins out of their native environment, affecting their function. Recently, a variety of synthetic polymers have been introduced, which can extract membrane proteins together with their native lipids into a so-called native nanodisc. However, they usually show lesser solubilization capacity than detergents, and their general applicability for membrane protein biochemistry is poorly understood. Here, we used Hek293 cell membrane extracts and LC-MS-based proteomics to compare the ability of nanodisc-forming polymers against state-of-the-art detergents to solubilize the membrane proteome. Our data demonstrates the general ability of synthetic co-polymers to extract membrane proteins, rivalling the efficacy of commonly used detergents. Interestingly, each class of solubilization agent presents specific solubilization profiles. Importantly, we found no correlation between efficiency and number of transmembrane domains, isoelectric point, or GRAVY score for any compound. Combined, our data show that these polymers are a versatile alternative to detergents for the biochemical and structural study of membrane proteins, functional proteomics or as components of a native lysis/solubilization buffers. Our work here represents the first attempt at a proteome-scale comparison of the efficacy of nanodisc-forming polymers. These data should serve as starting reference to researchers looking to purify membrane proteins in near native conditions.

Introduction

Integral membrane proteins perform key cellular functions, such as cell signaling, selective transport and generally they mediate the interaction between cells and their environment. Accordingly, although they represent about a quarter of all proteins encoded in the human genome (Fagerberg et al., 2010) they are the target of the majority of the currently approved drugs (Santos et al., 2017). Despite their clear relevance, they remain very poorly characterized. For instance, up until 2021, only 3% of all structures in the PDB were of membrane proteins (Le Bon et al., 2021). Many factors contribute to this, including low production yields, but perhaps the biggest challenge is that they need to be solubilized from the membrane. Traditionally, this is done using detergents, which remove the majority, if not all, lipids around the protein. Being stripped of their native environment, membrane proteins become usually unstable as lipids are known to be important co-factors for protein function and stability (Barrera et al., 2013; Bogdanov et al., 2008; Contreras et al., 2011; Laganowsky et al., 2014; Pollock et al., 2018; Saliba et al., 2015; Schmidpeter et al., 2022), and detergents can replace the lipid bilayers only to a very limited extent (Seddon et al., 2004). The choice of an appropriate detergent depends on the protein and the application. For example, quantitative and deep profiling of entire proteomes often requires either strong detergents such as sodium dodecylsulfate (SDS), sodium deoxycholate (SDC) or RapiGest™, high concentrations of chaotropic agents such as 8 M Urea or 6 M Guanidinium Hydrochloride, or mixture of them(Hughes et al., 2014; Vit et al., 2016; Wiśniewski et al., 2009). Furthermore, enrichment of membranes by ultracentrifugation followed by washing with alkaline sodium carbonate or 8 M Urea has been described to improve the identification of low abundant membrane proteins (Fujiki et al., 1982; Kongpracha et al., 2022). In the case of quantitative proteomics, highly denaturing extraction conditions are extremely helpful, since they instantly reduce intrinsic protease and phosphatase activity in extracts, disrupt supramolecular protein networks and unfold proteins making them amenable for efficient tryptic digestion. In clear contrast, structural and functional characterization requires proteins in near native state, and enzymatic activity as well molecular interactions should be preserved as far as possible. While many soluble proteins can be easily extracted in simple aqueous buffers, the addition of mild detergents such as decyl maltoside (DM), dodecyl maltoside (DDM) and lauryl maltose neopentyl glycol (LMNG) (Choy et al., 2021) is required for membrane proteins. To stabilize extracted membrane proteins, detergents must be kept above their critical micelle concentration (CMC) over the entire workflow, significantly increasing reagent costs, experiment complexity, and negatively affecting many downstream applications.

More than two decades ago, the group of Jean-Luc Popot (Tribet et al., 1996) developed a new kind of amphipathic polymers or "amphipols", capable of stabilizing integral membrane proteins. Amphipols can provide the hydrophobic environment the protein needs and bind it so tightly that no additional

amphipol or detergent is needed in downstream applications. For this reason, classical amphipols like A8-35, have been particularly popular for single particle electron cryo-microscopy (Cryo-EM) structures (Popot, 2018; Zoonens and Popot, 2014). Unfortunately, these polymers lack the ability to directly solubilize proteins from the membrane, and an initial detergent extraction is required. In 2009, the Overduin lab introduced a new class of co-polymer to tackle the challenge of solubilizing while preserving the native lipid environment (Knowles et al., 2009). Made by repeating units of styrene and maleic acid (SMA), SMAs were known to act as a molecular "cookie cutter" (Parmar et al., 2016) taking integral membrane proteins together with a belt of their own native lipids out of the membrane, forming a so-called SMALP (Styrene and Maleic acid lipid particle). To date, SMALPs have been used for many applications, including radioligand and spectroscopic binding assays, NMR based assays, and measurement of channel activity (see (Unger et al., 2021) for a summary). Unfortunately, SMALPs are unstable a pH values below 6.5, precipitate in the presence of divalent ions, and interfere with protein quantification using aromatic side chain absorption. However, in recent years, the promise of preserving the native lipid environment of the protein has led to the development of several alternative co-copolymers that tackled some of the shortcomings of the original SMAs (for an overview of this rapidly evolving field see (Brown et al., 2021; Krishnarjuna and Ramamoorthy, 2022; Orekhov et al., 2022)). Variations in composition and manufacturing processed generate polymers with distinct capabilities. For instance, replacing styrene by diisobutylene, Diisobutylene-maleic acid (DIBMA) produces a gentler polymer without absorption at 280 nm and higher tolerance to divalent ions (Oluwole et al., 2017). Although less efficient than SMAs, DIBMA could successfully solubilized ß2 adrenergic receptor producing a functional protein with higher stability compared to DDM (Harwood et al., 2021). Recently, two new polymer classes have been reported. Smith and colleagues (Smith et al., 2020) introduced a new co-polymers made of "acrylic acid and styrene" (AASTY) and synthesized by reversible addition-fragmentation chain-transfer. AASTYs have a much precisely controlled molecular weight and the use of acrylic acid confers them higher tolerance to divalent ions than SMAs (Timcenko et al., 2022). Interestingly, the group of Manuela Zoonens recently demonstrated that replacing the aliphatic group of traditional amphipols by cyclo-alkanes (CyclAPols, known commercially as Ultrasolute™ Amphipols) resulted in polymers with excellent solubilization characteristics, capable of forming native nanodiscs (Marconnet et al., 2020). Moreover, CyclAPols solubilized bateriorhodopsin shows increased thermal satiability when compared to SMAs.

Lipidomics analysis of SMAs and DIBMAs has demonstrated that both polymer classes can successfully extract native lipid from eukaryotic and bacterial cells, although the extracted lipidic composition is somehow dependent on the exact chemical nature of the polymer. Interestingly, the lipid composition of SMALPs depend also on the identity of the protein (Teo et al., 2019) suggesting that these polymers can capture local compositional variations of the membrane. For most of these polymers, high-

101 resolution Cryo-EM structure are available for membrane proteins solubilized from bacterial (Catalano
102 et al., 2021; Doyle et al., 2022; Flegler et al., 2020; Higgins et al., 2021; Qiu et al., 2018; Sun et al., 2018;
103 Swainsbury et al., 2023; Tascón et al., 2020) or eukaryotic cells (Yoder and Gouaux, 2020; Yu et al.,
104 2021), many of which showing densities consistent with the presence of native lipids (Catalano et al.,
105 2021; Doyle et al., 2022; Flegler et al., 2020; Qiu et al., 2018; Yoder and Gouaux, 2020). Unfortunately,
106 while there is clear evidence that all these polymers can form native nanodiscs, most of the information
107 about their solubilization capabilities come from selected example proteins and systematic
108 characterization of their solubilization capacity against other methods has only recently been
109 performed for SMA (Carlson et al., 2019; Morrison et al., 2021).

110 Here, we used LC-MS analysis to compare the ability of nanodisc-forming polymers and detergents to
111 extract membrane proteins from Hek293 cells. In contrast to in-depth characterization of selected
112 protein examples, shotgun proteomics facilitates the quantification of thousands of individual proteins
113 in parallel and allows for more generalized observations. Testing a total of 22 extraction conditions
114 including different types of SMAs, DIBMAs, AASTYs, and Ultrasolute™ Amphipol, and the commonly
115 used non-ionic detergents DM, DDM and LMNG, our data represents the most comprehensive
116 proteome-scale study on membrane protein solubilization by polymers.

117

118 **Methods**

119 **Cell culture**

120 Human embryonic kidney 293 cells (Expi293F™, Thermo Fisher) were cultured in Expi293™ Expression
121 medium at a cell density between 5 x 10^5 cells/ml and 4 x 10^6 cells/ml in suspension. 100 ml of a 2 x
122 10^6 cells/ ml culture growing in exponential phase were harvested by centrifugation and the cell pellet
123 was stored at – 80 °C.

124

125 **Preparation of membrane pellets**

126 The cell pellet was resuspended in 150 mM NaCl and 20 mM HEPES, pH 7.4, cells were disrupted by
127 sonication. After a centrifugation step at 9,000 x g the protein concentration of the supernatant was
128 adjusted to 0.25 mg/ml using 150 mM NaCl and 20 mM HEPES pH 7.4. The adjusted supernatant was
129 pipetted into 100µl aliquots, and the aliquots centrifuged at 60,000 x g for 1 hour. The supernatant was
130 discarded and the cell pellets consisting of approximately 25 µg of total proteins were frozen at - 80 °C.

131

132 **Protein extraction and digestion**

133 For an initial protein extraction screen SDS was tested as 5% solution in 50 mM HEPES pH 7.4. RIPA
134 buffer was composed of 150 mM NaCl, 1% Nonidet P-40, 0.5% deoxycholate, 0.1% SDS in 50 mM HEPES
135 pH 7.4. All other tested synthetic polymers and detergents were used as 2.5% solutions in 50 mM HEPES
136 pH 7.4 (Table 1). In a subsequent dilution experiment the extraction properties of a selected panel of
137 detergents and polymers were tested using five different concentrations ranging from 0.125% to 2.5%
138 in 50 mM HEPES pH 7.4 (Table 1). All reagent solutions and samples were used at 5° C and kept in pre-
139 chilled cooling racks. Either 25 µl detergent or polymer solution were added to the membrane pellets,
140 each containing approximately 25 µg total protein. The tubes were briefly vortexed and placed in a
141 Thermomixer (Eppendorf) for 16 h at 800 rpm and 5°C. After extraction, the tubes were transferred to
142 a pre-chilled rotor and centrifuged for 35 min at 21,000 x g and 5°C. 20 µl supernatant were carefully
143 transferred to new tubes without touching their bottom. 80 µl of cold acetone (-20°C) were added, the
144 tubes were briefly vortexed and incubated for 120 min at -20°C to precipitate proteins. Supernatants
145 were removed and the remaining protein pellets were washed once with 250 µl cold acetone (-20°). 25
146 µl 2% deoxycholate in 50 mM HEPES TrisHCl pH 8.5, 5 mM TCEP and 40 mM chloroacetamide were
147 added to the airdried protein pellets. Proteins were re-solubilized, reduced and S-alkylated in a single
148 step for 2 h at 46°C. 0.5 µg trypsin were added in 5 µl 2% deoxycholate in 50 mM TrisHCl pH 8.5 and
149 proteins were digested at 37°C. After 16 h, 30 µl of 5% trifluoroacetic acid were added to stop the

digest. By following this precipitation-resolubilization protocol, we removed solubilization agents and standardize the tryptic digestion step, which if fully compatible with SDC (Lin et al., 2008). Samples were centrifuged for 5 min at 21,000 x g and 20°C to pellet precipitated deoxycholate and 50 µl clear supernatant were removed and transferred to fresh tubes. 20 µl were subsequently loaded on DVB-RPS mixed mode stage tips activated with 20 µl methanol and equilibrated to 0.1% formic acid (FA). The loaded peptides were sequentially washed with 40 µl 0.1% FA in water and 40 µl 0.1% FA in 60% acetonitrile followed by alkaline elution with 40 µl 1% ammonium hydroxide in 60% acetonitrile. Eluates were immediately acidified with 10 µl 10% FA and dried in a vacuum centrifuge. Sample were re-solubilized in 10 µl 5% FA, 2% acetonitrile and stored at -20°C until LC-MS analysis.

LC-MS Data acquisition and processing

Protein digests were analyzed on a Q-Exactive Plus (Thermo Scientific) mass spectrometer that was coupled to an EASY nLC 1200 UPLC (Thermo Scientific). Re-solubilized protein digests were loaded onto an in-house-made pulled tip column (30 cm length, 75 µm inner diameter, filled with 2.7 µm Poroshell EC120 C18, Agilent) which has been equilibrated in 0.1% FA in water. Peptides were separated using increasing acetonitrile concentrations in 0.1% FA followed by a 10 min column wash with 95% acetonitrile in 0.1 % FA. 140 min gradients were used for data dependent (DDA) acquisitions and 90 min gradients with data independent (DIA) acquisitions. The protein extraction screen experiment was acquired with the DDA method. Briefly, MS1 survey scans were acquired from 300 to 1,750 m/z at a resolution of 70,000 and stored in profile mode. The top 10 most abundant peptides were isolated within a 1.8 Th window and subjected to HCD fragmentation at a normalized collision energy setting of 27%. The AGC target was set to 5e5 charges, allowing a maximum injection time of 60 ms. Product ions were detected in the Orbitrap at a resolution of 17,500. Precursors were dynamically excluded for 25 s. A DIA method was used for the analysis of the dilution experiment. MS1 scans were acquired from 380 m/z to 1,020 m/z at 35,000 resolution. Maximum injection time was set to 60 ms and the AGC target to 1E6. MS2 scans starting from 250 m/z were acquired with 17,500 resolution, maximum injection time of 60 ms and the AGC target set to 1E6. 30 x 20 m/z staggered DIA windows covered the precursor mass range from 400 m/z – 1,000 m/z and resulted in 60 nominal 10 m/z windows after deconvolution. For spectral library generation, aliquots of the 2.5% condition of all extraction experiments were pooled and analyzed with six consecutive gas phase fractionation (GPF) runs covering the mass range from 400 m/z to 1,000 m/z in sequential 100 m/z segments. MS2 scans were acquired with 25 x 4 m/z staggered windows in a 100 m/z range. All other settings were identical to the standard DIA method used for sample acquisition. DDA and DIA data were stored as centroid.

183

184 **Data analysis**

185 DDA runs were processed with MaxQuant version 1.5.3.8 (Tyanova et al., 2016a) using default
186 parameter. Briefly, MS2 spectra were searched against the human canonical swissprot reference
187 proteome database (UP5640, downloaded 08.26.2020), including a list of common contaminants. False
188 discovery rates on protein and PSM level were estimated by the target-decoy approach to 1% Protein
189 FDR and 1% PSM FDR respectively. The minimal peptide length was set to 7 amino acids and
190 carbamidomethylation at cysteine residues was considered as a fixed modification. Oxidation (M) and
191 Acetyl (Protein N-term) were included as variable modifications. The match-between runs option was
192 enabled within replicate groups. Protein and gene identifiers together with iBAQ intensities were
193 imported into Perseus version 1.6.5.0 (Tyanova et al., 2016b) for subsequent analysis. Decoys and
194 potential contaminants were removed. IBAQ values were log2 transformed and identified proteins
195 were filtered for at least 3 out of 3 values in at least one replicate group. Principal component analysis
196 was calculated on the imputed group means using Perseus defaults.

197 All DIA raw files were deconvoluted and transformed to mzML files using the msconvert module in
198 Proteowizard. DIA-NN 1.8.0 (Demichev et al., 2020) was used in library free mode to generate a project
199 specific spectral library from a human canonical Swissprot reference proteome fasta file and the 6 GPF
200 runs. The settings differing from defaults were: min precursor m/z set to 400, max precursor m/z set
201 to 1,000, min fragment m/z set to 250, max fragment m/z set to 1,800 and precursor charge states
202 ranging from 2 to 4. The resulting spectral library (11,214 proteins, 11,186 genes and 139,723
203 precursors) was used for the subsequent analysis of the sample runs with default parameters and the
204 relaxed protein inference option. Using the "diann" R-package (https://github.com/vdemichev/diann-
205 rpackage) MaxLFQ intensities were calculated from non-normalized intensities provided in the DIA-NN
206 output file and were imported into Perseus. For heatmap generation, data were filtered for at least 3
207 valid values in total and log2 transformed MaxLFQ values were normalized to an interval from 0-1.
208 Gravy Scores and Isoelectric points were calculated from the human canonical swissprot database
209 proteome (UP5640,) using the "Peptides" R-package (https://github.com/dosorio/Peptides/). Hek293
210 gene expression data were downloaded from https://www.proteinatlas.org (Uhlén et al., 2015). Entries
211 with noise level gene expression (TPM < 1) and non-membrane proteins (TMD count = 0) were
212 removed. The remaining entries were considered as expected membrane protein expression
213 background. Mean iBAQ intensities as well as protein level TMD counts were merged to the expression
214 background and the percentage of entries that were also identified by the proteomics experiment was
215 calculated to estimate the analytical depth of the proteomic analysis.

216 **Results and Discussion**

217 We used LC-MS to compare a panel of nanodisc-forming polymers and commonly used detergents for
218 their ability to extract integral transmembrane proteins from Hek293 cell membranes. In total 22
219 extraction conditions including different types of SMAs, DIBMAs, AASTYs, and Ultrasolute™, and the
220 commonly used non-ionic detergents DM, DDM and LMNG were tested. Our non-detergent control
221 was HEPES buffer. As positive control we chose SDS, SDC, and Fos-12 as a panel of very aggressive
222 detergents, as well as the ubiquitously used RIPA buffer. While these are not suited for native
223 extraction, their high protein solubilization capacity should provide an upper limit of detectable
224 membrane proteins in the current experimental setup. For an overview of the compounds tested (Table
225 1) and their physicochemical characteristics see Table S1.

226

227 **Analytical depth of our study**

228 We could identify a total of 7,197 proteins across all runs, including 5,665 non-membrane proteins
229 (Table S2). We attribute this to loosely membrane-interacting proteins or soluble proteins trapped in
230 vesicles. Normally, this is dealt by washing the samples with alkaline carbonate buffers(Fujiki et al.,
231 1982; Kongpracha et al., 2022). However, the elevated pH needed for this (> 11) is incompatible with
232 native protein extraction. Therefore, we filtered the data for proteins with at least one TMD, leaving
233 1,532 membrane protein identifications. For comparison, RNA-seq experiments of Hek293 cells report
234 2,371 transmembrane proteins to be expressed with transcript levels greater 1 transcript per million
235 (Protein Atlas; https://www.proteinatlas.org/). Considering this number as expression background, we
236 estimated the analytical depth of our proteome analysis to be better than 64 % for proteins with at
237 least one TMD. Importantly, while mRNA levels are not always good predictors with protein amounts,
238 they should be strongly correlated for the cell growth conditions we tested (Liu et al., 2016). Indeed,
239 comparing transcript levels with our detected proteins (Figure S1), suggests that low gene expression
240 is the major reason for proteins missing in our data set, strongly arguing for the high quality of the
241 dataset.

242

243 **Different solubilization compounds results in unique solubilization patterns**

244 For our initial screening round, we assessed the solubilization capacity of all compounds at a final
245 concentration of 2.5%, or 5% in the case of SDS. To get an initial overview of their solubilization
246 differences, we used the mean abundance of the detected membrane proteins to performed a
247 principal component analysis (PCA). Strikingly, the first two components (~70% of the variance) reveal

248 that individual reagents form tight cluster with other members of their respective classes (Figure 1A).
249 Higher components can separate ionic from non-ionic detergents, while to a lesser extent still
250 preserving the separate clustering of the different polymer classes (Figure 1B)

251 The clear separation between detergents and polymers, as well as the separation between different
252 polymer classes suggest that each solubilization agent class produces its own distinctive fingerprint.
253 However, a relation between the individual components of the PCA and specific physicochemical
254 characteristics of the compounds is not immediately obvious. To our surprise, although denaturation
255 potential and extraction properties of ionic and non-ionic detergents are clearly different, DM, DDM
256 and LMNG cluster closely with the much more aggressive SDS, SDC and Fos-12. As expected, the RIPA
257 buffer — a mixture of SDS, SDC and Nonidet P-40 (NP-40) — is located within this cluster as well.
258 Digitonin does not follow this trend, and is located far away from the main detergent cluster, near SMA
259 502-E.

260

261 **Polymers can efficiently solubilize membrane proteins**

262 Next, we sought to understand whether the differences in solubilization profiles we observe are a
263 consequence of differences in solubilization efficiency or versatility. In our negative control, we
264 detected an average of 253 membrane proteins, 181 (71.41%) of which are single span membrane
265 proteins (Figure 2). In clear contrast, the membrane protein counts for the ionic detergents SDC, SDS
266 and Fos-12 were 1250, 1,241, and 1,280 respectively. Unexpectedly, the ionic detergents performed
267 similarly to Ultrasolute™ Amphipol-17 and Amphipol-18 (1,270 and 1,272 membrane proteins
268 respectively) and were outperformed by the non-ionic detergents DM, DDM, and LMNG (membrane
269 protein counts of 1,297, 1,308, and 1,315 respectively); the latter being the highest in the data set
270 (Figure 2). We obtained intermediate efficiency for SMAs, with counts of 1,175, 1,198 and 1,066 for
271 SMA-200, SMA-300 and SMA-502-E respectively. AASTYs and the DIBMAs had the lowest performance
272 with counts ranging from 991 to 1,010 and from 897 to 969 respectively (Figure 2). Nevertheless,
273 DIBMAs and AASTYs are efficient solubilization agents, showing significantly higher solubilization than
274 the background HEPES alone. Importantly, solubilization efficiency of membrane proteins is only one
275 piece of the puzzle. Purification strategy, stabilization of the membrane protein and downstream
276 applications are equally important aspects to consider, which makes screening of various reagents
277 indispensable. Indeed, polymer identity or even concentration can affect all of these parameters
278 (Szundi et al., 2021). Absolute solubilization efficiency may also not be critical for many applications
279 where a near-native state is the strongest constraint and sufficient initial material is present; the
280 obvious example would be after overexpression. For instance, the comparably milder DIBMA has been

281 successfully used to determine the Cryo-EM structure of the mechanosensitive-like channel YnaI
282 (Flegler et al., 2020) and has been successfully used to produce highly active and stable GPCR samples
283 (Harwood et al., 2021).

284

285 **Polymers can efficiently extract diverse classes of membrane proteins**

286 Our PCA analysis revealed that different compound classes we tested produce distinct solubilization
287 patterns. Although they clearly differ in their solubilization efficiency, this cannot be the only driver as
288 the clustering of detergent and polymer classes remains present for higher components in the PCA
289 analysis (Figure 1B). We first analyzed the potential impact of the membrane protein topology on
290 solubilization. For this, we grouped proteins according to their number of TMDs and calculated
291 identification rates as the fraction of membrane proteins we identified versus what we expected from
292 RNA data. Identification rate differs substantially among TMD groups (Figure 3). Interestingly, the
293 profiles are similar for all tested extraction conditions, with scale differences clearly proportional to
294 efficiency. Since median protein abundancies have a major impact on identification rates in proteomic
295 experiments, we tested if this was behind the identification rate pattern. Indeed, mRNA level shows a
296 similar pattern to our detection rates (Figure 3), with a significant correlation between identification
297 rates and median mRNA abundance (Figure S1). In turn this suggests that protein abundance and not
298 preferential solubilization is behind the identification rate pattern.

299 A clear candidate for the differential polymer preferences would be the physicochemical properties of
300 the proteins and their respective transmembrane regions. For instance, hydrophobicity and charge
301 substantially differ across membrane proteins and could easily affect the polymer's solubilization
302 efficiency. To test this, we calculated GRAVY scores and isoelectric points for either the full protein
303 sequences or their membrane spanning regions. Interestingly, the distributions of either characteristic
304 for the detected membrane proteins reveal no major difference among the solubilization agents,
305 strongly suggesting that isoelectric points and hydrophobicity cannot explain the differential extraction
306 patterns and that we observe (Figure 4).

307 Contrary to detergents, the polymers we tested solubilize the protein together with its lipidic
308 microenvironment. Far from being just a scaffold for these proteins, the exact lipidic around them is
309 matched to their specific requirements (Lee, 2004), with each of them possessing their own lipidic
310 fingerprint (Corradi et al., 2018). Interestingly, SMAs have already been shown to solubilize, from the
311 same membrane, proteins with different local lipidic composition (Teo et al., 2019). However, early
312 characterization of nanodisc-forming polymers has shown that their solubilization efficiency is
313 somehow dependent on membrane composition (Oluwole et al., 2017; Smith et al., 2020). Combined,

314 this suggests that, for a specific target, differences in solubilization ability between polymers would be
315 partially determined by the identity of the annular lipids surrounding the membrane protein.

316

317 **Optimal solubilization conditions are specific to each compound and target combination**

318 So far, we compared the capacity of polymers and detergents to extract membrane proteins using a
319 standard concentration of 2.5%. Although this concentration is effective for all conditions tested, it is
320 relatively high. In many cases, high concentrations like these can interfere with purification, or affect
321 the activity of the protein (Szundi et al., 2021). In those kinds of cases where gentle solubilization of
322 proteins is required, it is common practice to use additives at concentrations as low as possible in order
323 to minimize detrimental effects. DDM and LMNG are typically used from 0.1% to 1%**,** whereas SMAs
324 have been successfully used in concentrations as low as 0.25% (Kopf et al., 2020; Pitch et al., 2021). In
325 order to determine useful minimal concentrations, we performed a second extraction screen with
326 concentrations of 0.125%, 0.25%, 0.5%, 1% and 2.5% for a selected panel of polymers and non-ionic
327 detergents. The raw data from this experiment can be found in Table S2**.** In line with the first screening,
328 DDM and LMNG were the most efficient compounds and reached maximum membrane protein counts
329 at concentrations as low as 0.5% (Figure 5A) and maximum summed intensities at 1% (Figure 5B). In
330 agreement with our earlier experiments, Ultrasolute™ Amphipol-17 and 18 showed very high
331 solubilization efficiency reaching their maximum counts at 1% and plateauing at a maximum value of
332 summed intensities comparable to detergents. AASTY 11-45 and 6-50 also reached a plateau for
333 summed intensities at concentrations above 1%, although only AASTY 11-45 does not seem to find a
334 plateau for the number of individual membrane proteins (Figure 5A,B). DIBMAs in general seem to find
335 a plateau for both quantities, although with much lower values (Figure 5A,B), arguing for a generally
336 lower solubilization efficiency. For all other compounds the curves imply that the concentration for
337 maximum solubilization has not been reached and may clearly exceed 2.5%. Combined, this shows that
338 polymers can be efficiently used at concentrations significantly lower than 2.5%. We would recommend
339 0.25 – 1% for Ultrasolute™ Amphipols and 0.5 – 1% for AASTYs, while a higher concentration would be
340 required for DIBMAs and SMAs. To what extent these results from endogenously expressed targets in
341 this study can be transferred to overexpression conditions has to be tested individually for each target.

342 Finally, to further dissect the versatility of these polymers we created a heatmap of the normalized
343 protein intensities obtained for each individual detected membrane proteins, at each different
344 solubilization agent concentration (Figure 6). Unsurprisingly, detergents are able to solubilize most of
345 the proteins in the map with high efficiency. In addition, Ultrasolute™ Amphipols and to a lesser extent
346 AASTY 6-50 produce a very similar patter, both in terms of concentration dependency and number and

347 identity of the solubilized proteins. Combined this demonstrates that nanodisc-forming polymers
348 present a strong alternative to detergents, especially when the lipid environment is key for protein
349 function.

350

351 **Concluding remarks**

352 We used LC-MS to perform label-free quantification proteomics aimed at screening native-nanodisc-
353 forming polymers and compared them with state-of-the-art detergents for their ability to solubilize the
354 Hek293 membrane proteome. We omitted other membrane-mimetic strategies — such as MSP-based
355 nanodisc (Bayburt et al., 2002), peptidisc (Carlson et al., 2018) and saponins (Frauenfeld et al., 2016)
356 — as they all require the intermediate addition of detergents, thus altering the native environment of
357 the proteins under investigation. The study presented here is the first major attempt to compare the
358 ability of a comprehensive panel of polymers at the proteome scale. As such, we believe that this study
359 will become a reference for researches working with different aspects of the biochemistry of
360 membrane proteins.

361 We have demonstrated that these synthetic polymers exhibit solubilization performance that can rival
362 those observed in commonly used detergents, but have the advantage of preserving the protein in a
363 near-native environment; Ultrasolute™ Amphiphol 17 and 18 even outperformed the denaturing
364 detergent group. Considering the separate clustering observed in Figure 1, plus the patterns observed
365 in Figure 6, we believe that, for any given target, it is likely that at least one polymer class should provide
366 efficient solubilizationWe are certain being able to preserve the native membrane environment will
367 become and invaluable tool for membrane biochemists. As such, we anticipate that these synthetic
368 polymers will have a broad range of application in the future, in particular as components of native
369 lysis and solubilization buffers. Moreover, with the ever-increasing access the electron cryo-microscopy
370 we expect that these polymers will make a big impact in the structural biology of integral membrane
371 proteins.

372

373

Acknowledgements

All mass spectrometric analysis was performed in the CMMC/CECAD Proteomics Facility, CECAD University of Cologne.

Data Availability

The mass spectrometry data included in this manuscript is available in Table S2. For ease of navigation, we have also created a solubilization database with the data from the manuscript, available at https://cube-biotech.com/solubilization-database

Conflict of interest disclosure

JK, BM, PH, and FM are shareholders of Cube Biotech GmbH, which produces and sells synthetic co-polymers for membrane protein characterization. SM and JWL declare no conflict of interest.

388 **References**

389 Barrera, N.P., Zhou, M., Robinson, C.V., 2013. The role of lipids in defining membrane protein
390 interactions: insights from mass spectrometry. Trends Cell Biol. 23, 1–8.
391 https://doi.org/10.1016/j.tcb.2012.08.007

392 Bogdanov, M., Mileykovskaya, E., Dowhan, W., 2008. Lipids in the Assembly of Membrane Proteins and
393 Organization of Protein Supercomplexes. Subcell. Biochem. 49, 197–239. https://doi.org/10.1007/978-
394 1-4020-8831-5_8

395 Brown, C.J., Trieber, C., Overduin, M., 2021. Structural biology of endogenous membrane protein
396 assemblies in native nanodiscs. Curr. Opin. Struct. Biol. 69, 70–77.
397 https://doi.org/10.1016/j.sbi.2021.03.008

398 Carlson, M.L., Stacey, R.G., Young, J.W., Wason, I.S., Zhao, Z., Rattray, D.G., Scott, N., Kerr, C.H., Babu,
399 M., Foster, L.J., Duong Van Hoa, F., 2019. Profiling the Escherichia coli membrane protein interactome
400 captured in Peptidisc libraries. eLife 8, e46615. https://doi.org/10.7554/eLife.46615

401 Catalano, C., Ben-Hail, D., Qiu, W., Blount, P., des Georges, A., Guo, Y., 2021. Cryo-EM Structure of
402 Mechanosensitive Channel YnaI Using SMA2000: Challenges and Opportunities. Membranes 11, 849.
403 https://doi.org/10.3390/membranes11110849

404 Choy, B.C., Cater, R.J., Mancia, F., Pryor, E.E., 2021. A 10-year meta-analysis of membrane protein
405 structural biology: Detergents, membrane mimetics, and structure determination techniques. Biochim.
406 Biophys. Acta BBA - Biomembr. 1863, 183533. https://doi.org/10.1016/j.bbamem.2020.183533

407 Contreras, F.-X., Ernst, A.M., Wieland, F., Brügger, B., 2011. Specificity of Intramembrane Protein–Lipid
408 Interactions. Cold Spring Harb. Perspect. Biol. 3, a004705.
409 https://doi.org/10.1101/cshperspect.a004705

410 Corradi, V., Mendez-Villuendas, E., Ingólfsson, H.I., Gu, R.-X., Siuda, I., Melo, M.N., Moussatova, A.,
411 DeGagné, L.J., Sejdiu, B.I., Singh, G., Wassenaar, T.A., Delgado Magnero, K., Marrink, S.J., Tieleman, D.P.,
412 2018. Lipid–Protein Interactions Are Unique Fingerprints for Membrane Proteins. ACS Cent. Sci. 4, 709–
413 717. https://doi.org/10.1021/acscentsci.8b00143

414 Demichev, V., Messner, C.B., Vernardis, S.I., Lilley, K.S., Ralser, M., 2020. DIA-NN: neural networks and
415 interference correction enable deep proteome coverage in high throughput. Nat. Methods 17, 41–44.
416 https://doi.org/10.1038/s41592-019-0638-x

417 Doyle, M.T., Jimah, J.R., Dowdy, T., Ohlemacher, S.I., Larion, M., Hinshaw, J.E., Bernstein, H.D., 2022.
418 Cryo-EM structures reveal multiple stages of bacterial outer membrane protein folding. Cell 185, 1143-
419 1156.e13. https://doi.org/10.1016/j.cell.2022.02.016

420 Flegler, V.J., Rasmussen, A., Rao, S., Wu, N., Zenobi, R., Sansom, M.S.P., Hedrich, R., Rasmussen, T.,
421 Böttcher, B., 2020. The MscS-like channel YnaI has a gating mechanism based on flexible pore helices.
422 Proc. Natl. Acad. Sci. 117, 28754–28762. https://doi.org/10.1073/pnas.2005641117

423 Fujiki, Y., Hubbard, A.L., Fowler, S., Lazarow, P.B., 1982. Isolation of intracellular membranes by means
424 of sodium carbonate treatment: application to endoplasmic reticulum. J. Cell Biol. 93, 97–102.
425 https://doi.org/10.1083/jcb.93.1.97

426 Harwood, C.R., Sykes, D.A., Hoare, B.L., Heydenreich, F.M., Uddin, R., Poyner, D.R., Briddon, S.J.,
427 Veprintsev, D.B., 2021. Functional solubilization of the β2-adrenoceptor using diisobutylene maleic
428 acid. iScience 24. https://doi.org/10.1016/j.isci.2021.103362

429 Higgins, A.J., Flynn, A.J., Marconnet, A., Musgrove, L.J., Postis, V.L.G., Lippiat, J.D., Chung, C., Ceska, T.,
430 Zoonens, M., Sobott, F., Muench, S.P., 2021. Cycloalkane-modified amphiphilic polymers provide direct
431 extraction of membrane proteins for CryoEM analysis. Commun. Biol. 4, 1–9.
432 https://doi.org/10.1038/s42003-021-02834-3

433 Hughes, C.S., Foehr, S., Garfield, D.A., Furlong, E.E., Steinmetz, L.M., Krijgsveld, J., 2014. Ultrasensitive
434 proteome analysis using paramagnetic bead technology. Mol. Syst. Biol. 10, 757.
435 https://doi.org/10.15252/msb.20145625

436 Knowles, T.J., Finka, R., Smith, C., Lin, Y.-P., Dafforn, T., Overduin, M., 2009. Membrane Proteins
437 Solubilized Intact in Lipid Containing Nanoparticles Bounded by Styrene Maleic Acid Copolymer. J. Am.
438 Chem. Soc. 131, 7484–7485. https://doi.org/10.1021/ja810046q

439 Kongpracha, P., Wiriyasermkul, P., Isozumi, N., Moriyama, S., Kanai, Y., Nagamori, S., 2022. Simple But
440 Efficacious Enrichment of Integral Membrane Proteins and Their Interactions for In-Depth Membrane
441 Proteomics. Mol. Cell. Proteomics 21. https://doi.org/10.1016/j.mcpro.2022.100206

442 Kopf, A.H., Dörr, J.M., Koorengevel, M.C., Antoniciello, F., Jahn, H., Killian, J.A., 2020. Factors influencing
443 the solubilization of membrane proteins from Escherichia coli membranes by styrene–maleic acid
444 copolymers. Biochim. Biophys. Acta BBA - Biomembr. 1862, 183125.
445 https://doi.org/10.1016/j.bbamem.2019.183125

446 Krishnarjuna, B., Ramamoorthy, A., 2022. Detergent-Free Isolation of Membrane Proteins and
447 Strategies to Study Them in a Near-Native Membrane Environment. Biomolecules 12, 1076.
448 https://doi.org/10.3390/biom12081076

449 Laganowsky, A., Reading, E., Allison, T.M., Ulmschneider, M.B., Degiacomi, M.T., Baldwin, A.J., Robinson,
450 C.V., 2014. Membrane proteins bind lipids selectively to modulate their structure and function. Nature
451 510, 172–175. https://doi.org/10.1038/nature13419

452 Le Bon, C., Michon, B., Popot, J.-L., Zoonens, M., 2021. Amphipathic environments for determining the
453 structure of membrane proteins by single-particle electron cryo-microscopy. Q. Rev. Biophys. 54, e6.
454 https://doi.org/10.1017/S0033583521000044

455 Lee, A.G., 2004. How lipids affect the activities of integral membrane proteins. Biochim. Biophys. Acta
456 BBA - Biomembr. 1666, 62–87. https://doi.org/10.1016/j.bbamem.2004.05.012

457 Lin, Y., Zhou, J., Bi, D., Chen, P., Wang, X., Liang, S., 2008. Sodium-deoxycholate-assisted tryptic digestion
458 and identification of proteolytically resistant proteins. Anal. Biochem. 377, 259–266.
459 https://doi.org/10.1016/j.ab.2008.03.009

460 Liu, Y., Beyer, A., Aebersold, R., 2016. On the Dependency of Cellular Protein Levels on mRNA
461 Abundance. Cell 165, 535–550. https://doi.org/10.1016/j.cell.2016.03.014

462 Marconnet, A., Michon, B., Le Bon, C., Giusti, F., Tribet, C., Zoonens, M., 2020. Solubilization and
463 Stabilization of Membrane Proteins by Cycloalkane-Modified Amphiphilic Polymers.
464 Biomacromolecules 21, 3459–3467. https://doi.org/10.1021/acs.biomac.0c00929

465 Morrison, K.A., Heesom, K.J., Edler, K.J., Doutch, J., Price, G.J., Koumanov, F., Whitley, P., 2021.
466 Development of Methodology to Investigate the Surface SMALPome of Mammalian Cells. Front. Mol.
467 Biosci. 8.

468 Oluwole, A.O., Danielczak, B., Meister, A., Babalola, J.O., Vargas, C., Keller, S., 2017. Solubilization of
469 Membrane Proteins into Functional Lipid-Bilayer Nanodiscs Using a Diisobutylene/Maleic Acid
470 Copolymer. Angew. Chem. Int. Ed. 56, 1919–1924. https://doi.org/10.1002/anie.201610778

471 Orekhov, P.S., Bozdaganyan, M.E., Voskoboynikova, N., Mulkidjanian, A.Y., Karlova, M.G., Yudenko, A.,
472 Remeeva, A., Ryzhykau, Y.L., Gushchin, I., Gordeliy, V.I., Sokolova, O.S., Steinhoff, H.-J., Kirpichnikov,
473 M.P., Shaitan, K.V., 2022. Mechanisms of Formation, Structure, and Dynamics of Lipoprotein Discs
474 Stabilized by Amphiphilic Copolymers: A Comprehensive Review. Nanomaterials 12, 361.
475 https://doi.org/10.3390/nano12030361

476 Parmar, M.J., Lousa, C.D.M., Muench, S.P., Goldman, A., Postis, V.L.G., 2016. Artificial membranes for
477 membrane protein purification, functionality and structure studies. Biochem. Soc. Trans. 44, 877–882.
478 https://doi.org/10.1042/BST20160054

479 Pitch, S.G., Yao, W., Szundi, I., Fay, J., Chen, E., Shumate, A., Kliger, D.S., Farrens, D.L., 2021. Functional
480 integrity of membrane protein rhodopsin solubilized by styrene-maleic acid copolymer. Biophys. J. 120,
481 3508–3515. https://doi.org/10.1016/j.bpj.2021.05.008

482 Pollock, N.L., Lee, S.C., Patel, J.H., Gulamhussein, A.A., Rothnie, A.J., 2018. Structure and function of
483 membrane proteins encapsulated in a polymer-bound lipid bilayer. Biochim. Biophys. Acta BBA -
484 Biomembr., Beyond the Structure-Function Horizon of Membrane Proteins 1860, 809–817.
485 https://doi.org/10.1016/j.bbamem.2017.08.012

486 Popot, J.-L., 2018. Membrane Proteins in Aqueous Solutions, Biological and Medical Physics, Biomedical
487 Engineering. Springer International Publishing, Cham. https://doi.org/10.1007/978-3-319-73148-3

488 Qiu, W., Fu, Z., Xu, G.G., Grassucci, R.A., Zhang, Y., Frank, J., Hendrickson, W.A., Guo, Y., 2018. Structure
489 and activity of lipid bilayer within a membrane-protein transporter. Proc. Natl. Acad. Sci. 115, 12985–
490 12990. https://doi.org/10.1073/pnas.1812526115

491 Saliba, A.-E., Vonkova, I., Gavin, A.-C., 2015. The systematic analysis of protein–lipid interactions comes
492 of age. Nat. Rev. Mol. Cell Biol. 16, 753–761. https://doi.org/10.1038/nrm4080

493 Santos, R., Ursu, O., Gaulton, A., Bento, A.P., Donadi, R.S., Bologa, C.G., Karlsson, A., Al-Lazikani, B.,
494 Hersey, A., Oprea, T.I., Overington, J.P., 2017. A comprehensive map of molecular drug targets. Nat. Rev.
495 Drug Discov. 16, 19–34. https://doi.org/10.1038/nrd.2016.230

496 Schmidpeter, P.A.M., Wu, D., Rheinberger, J., Riegelhaupt, P.M., Tang, H., Robinson, C.V., Nimigean,
497 C.M., 2022. Anionic lipids unlock the gates of select ion channels in the pacemaker family. Nat. Struct.
498 Mol. Biol. 1–9. https://doi.org/10.1038/s41594-022-00851-2

499 Seddon, A.M., Curnow, P., Booth, P.J., 2004. Membrane proteins, lipids and detergents: not just a soap
500 opera. Biochim. Biophys. Acta BBA - Biomembr., Lipid-Protein Interactions 1666, 105–117.
501 https://doi.org/10.1016/j.bbamem.2004.04.011

502 Smith, A.A.A., Autzen, H.E., Faust, B., Mann, J.L., Muir, B.W., Howard, S., Postma, A., Spakowitz, A.J.,
503 Cheng, Y., Appel, E.A., 2020. Lipid Nanodiscs via Ordered Copolymers. Chem 6, 2782–2795.
504 https://doi.org/10.1016/j.chempr.2020.08.004

505 Sun, C., Benlekbir, S., Venkatakrishnan, P., Wang, Y., Hong, S., Hosler, J., Tajkhorshid, E., Rubinstein, J.L.,
506 Gennis, R.B., 2018. Structure of the alternative complex III in a supercomplex with cytochrome oxidase.
507 Nature 557, 123–126. https://doi.org/10.1038/s41586-018-0061-y

508 Swainsbury, D.J.K., Hawkings, F.R., Martin, E.C., Musiał, S., Salisbury, J.H., Jackson, P.J., Farmer, D.A.,
509 Johnson, M.P., Siebert, C.A., Hitchcock, A., Hunter, C.N., 2023. Cryo-EM structure of the four-subunit
510 Rhodobacter sphaeroides cytochrome bc1 complex in styrene maleic acid nanodiscs. Proc. Natl. Acad.
511 Sci. 120, e2217922120. https://doi.org/10.1073/pnas.2217922120

Szundi, I., Pitch, S.G., Chen, E., Farrens, D.L., Kliger, D.S., 2021. Styrene-maleic acid copolymer effects on the function of the GPCR rhodopsin in lipid nanoparticles. Biophys. J. 120, 4337–4348. https://doi.org/10.1016/j.bpj.2021.09.012

Tascón, I., Sousa, J.S., Corey, R.A., Mills, D.J., Griwatz, D., Aumüller, N., Mikusevic, V., Stansfeld, P.J., Vonck, J., Hänelt, I., 2020. Structural basis of proton-coupled potassium transport in the KUP family. Nat. Commun. 11, 626. https://doi.org/10.1038/s41467-020-14441-7

Teo, A.C.K., Lee, S.C., Pollock, N.L., Stroud, Z., Hall, S., Thakker, A., Pitt, A.R., Dafforn, T.R., Spickett, C.M., Roper, D.I., 2019. Analysis of SMALP co-extracted phospholipids shows distinct membrane environments for three classes of bacterial membrane protein. Sci. Rep. 9, 1813. https://doi.org/10.1038/s41598-018-37962-0

Timcenko, M., Autzen, A.A.A., Autzen, H.E., 2022. Characterization of Divalent Cation Interactions with AASTY Nanodiscs. ACS Appl. Polym. Mater. 4, 1071–1083. https://doi.org/10.1021/acsapm.1c01507

Tribet, C., Audebert, R., Popot, J.-L., 1996. Amphipols: Polymers that keep membrane proteins soluble in aqueous solutions. Proc. Natl. Acad. Sci. 93, 15047–15050. https://doi.org/10.1073/pnas.93.26.15047

Tyanova, S., Temu, T., Cox, J., 2016a. The MaxQuant computational platform for mass spectrometry-based shotgun proteomics. Nat. Protoc. 11, 2301–2319. https://doi.org/10.1038/nprot.2016.136

Tyanova, S., Temu, T., Sinitcyn, P., Carlson, A., Hein, M.Y., Geiger, T., Mann, M., Cox, J., 2016b. The Perseus computational platform for comprehensive analysis of (prote)omics data. Nat. Methods 13, 731–740. https://doi.org/10.1038/nmeth.3901

Uhlén, M., Fagerberg, L., Hallström, B.M., Lindskog, C., Oksvold, P., Mardinoglu, A., Sivertsson, Å., Kampf, C., Sjöstedt, E., Asplund, A., Olsson, I., Edlund, K., Lundberg, E., Navani, S., Szigyarto, C.A.-K., Odeberg, J., Djureinovic, D., Takanen, J.O., Hober, S., Alm, T., Edqvist, P.-H., Berling, H., Tegel, H., Mulder, J., Rockberg, J., Nilsson, P., Schwenk, J.M., Hamsten, M., von Feilitzen, K., Forsberg, M., Persson, L., Johansson, F., Zwahlen, M., von Heijne, G., Nielsen, J., Pontén, F., 2015. Tissue-based map of the human proteome. Science 347, 1260419. https://doi.org/10.1126/science.1260419

Unger, L., Ronco-Campaña, A., Kitchen, P., Bill, R.M., Rothnie, A.J., 2021. Biological insights from SMA-extracted proteins. Biochem. Soc. Trans. 49, 1349–1359. https://doi.org/10.1042/BST20201067

Vit, O., Man, P., Kadek, A., Hausner, J., Sklenar, J., Harant, K., Novak, P., Scigelova, M., Woffendin, G., Petrak, J., 2016. Large-scale identification of membrane proteins based on analysis of trypsin-protected transmembrane segments. J. Proteomics 149, 15–22. https://doi.org/10.1016/j.jprot.2016.03.016

Wiśniewski, J.R., Zougman, A., Nagaraj, N., Mann, M., 2009. Universal sample preparation method for proteome analysis. Nat. Methods 6, 359–362. https://doi.org/10.1038/nmeth.1322

Yoder, N., Gouaux, E., 2020. The His-Gly motif of acid-sensing ion channels resides in a reentrant 'loop' implicated in gating and ion selectivity. eLife 9, e56527. https://doi.org/10.7554/eLife.56527

Yu, J., Zhu, H., Lape, R., Greiner, T., Du, J., Lü, W., Sivilotti, L., Gouaux, E., 2021. Mechanism of gating and partial agonist action in the glycine receptor. Cell 184, 957-968.e21. https://doi.org/10.1016/j.cell.2021.01.026

Zoonens, M., Popot, J.-L., 2014. Amphipols for Each Season. J. Membr. Biol. 247, 759–796. https://doi.org/10.1007/s00232-014-9666-8

554 **Figures**

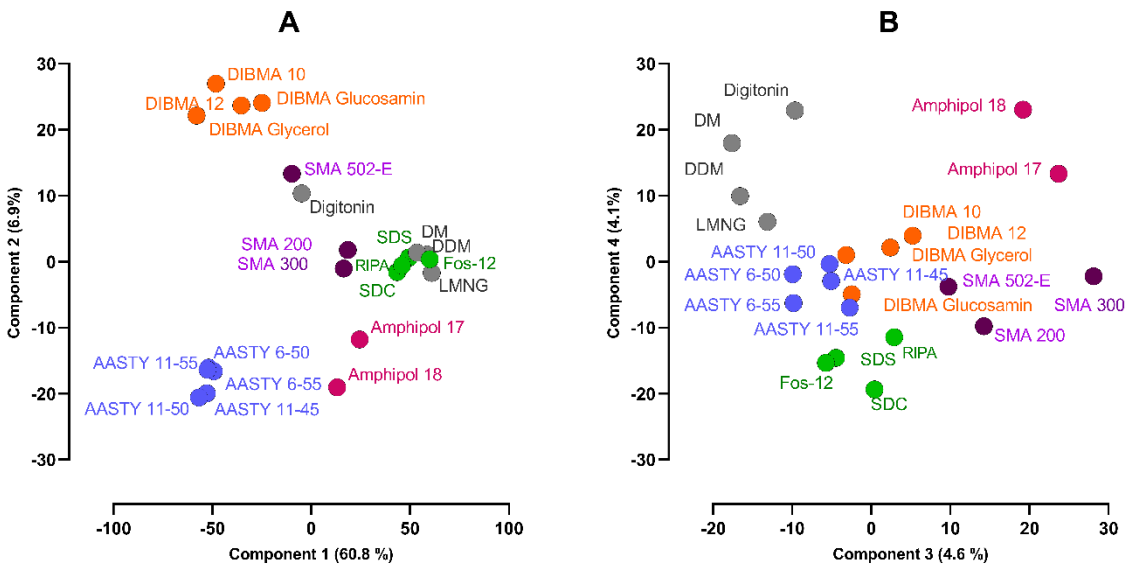

555

556 **Figure 1. Clustering of membrane protein extraction profiles of different solubilization agents.**
557 Principal component analysis of the membrane protein iBAQ values. The means of three replicates per
558 extraction condition were used. Each class of solubilization agent is shown in a different color to
559 highlight their clustering.

560

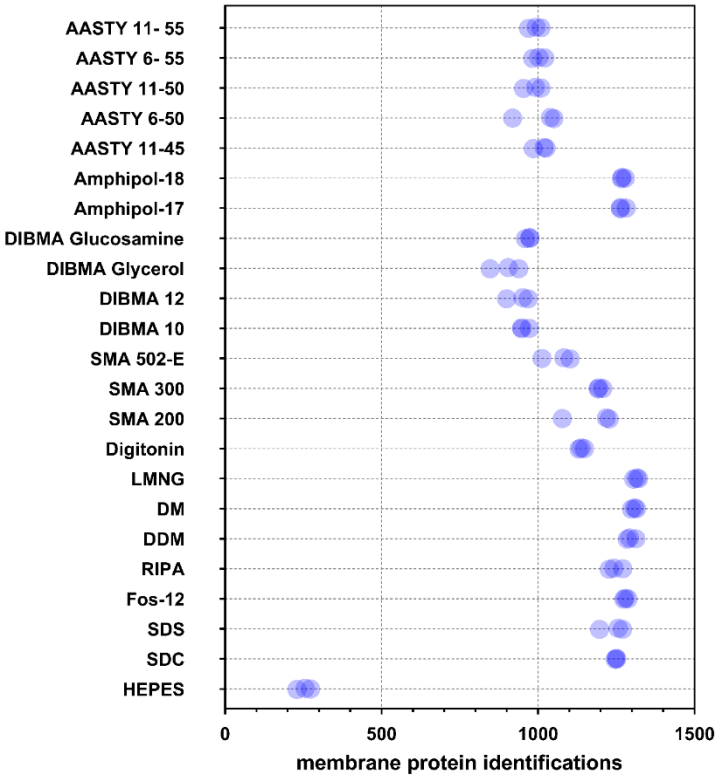

Figure 2. Cumulative number of detected membrane proteins. For each replicate and condition, the summed number of membrane protein identifications is shown.

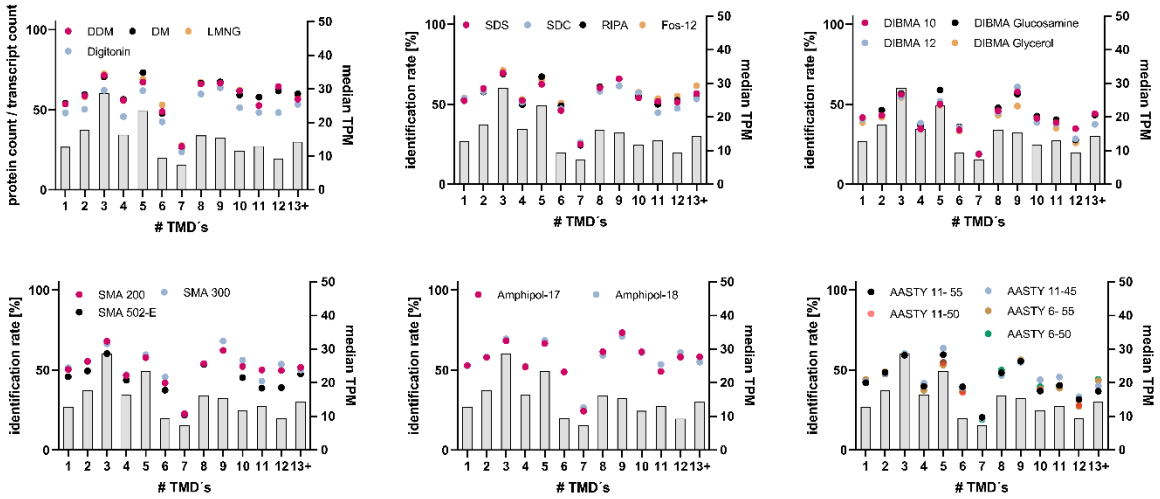

Figure 3. Membrane protein identification rate as a function of the number transmembrane domains. For each solubilization agent class, we calculate the identification rate as fraction of identified membrane proteins versus the total number of expressed membrane proteins in Hek293 cells. We further subdivided the proteins according to their number of transmembrane domains. For reference, we also plotted the RNA level as median number of transcripts per million in grey bars.

596

597

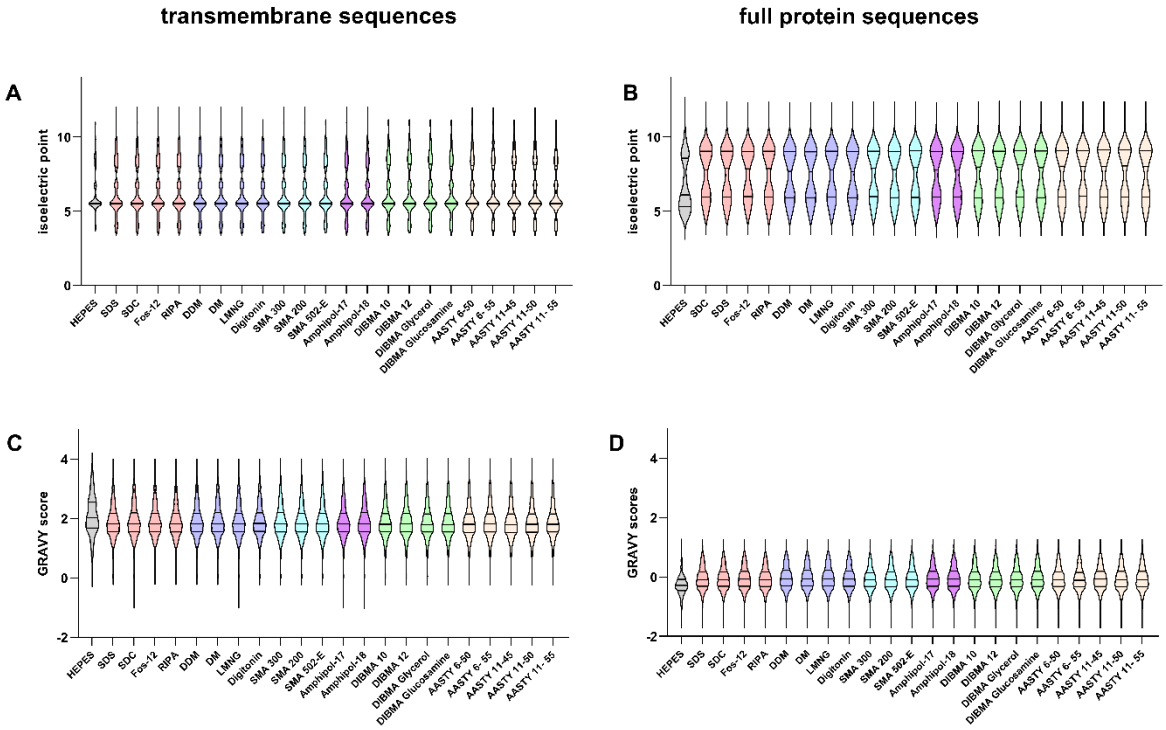

598

599 **Figure 4. Distribution of isoelectric points and GRAVY scores for the proteins detected in our**
600 **solubilization experiments.** For all detected membrane proteins we calculated the isoelectric points
601 (**A,B**) and GRAVY scores (**C,D**) using either the transmembrane regions (**A,C**) or the full protein
602 sequence (**B,D**).

603

604

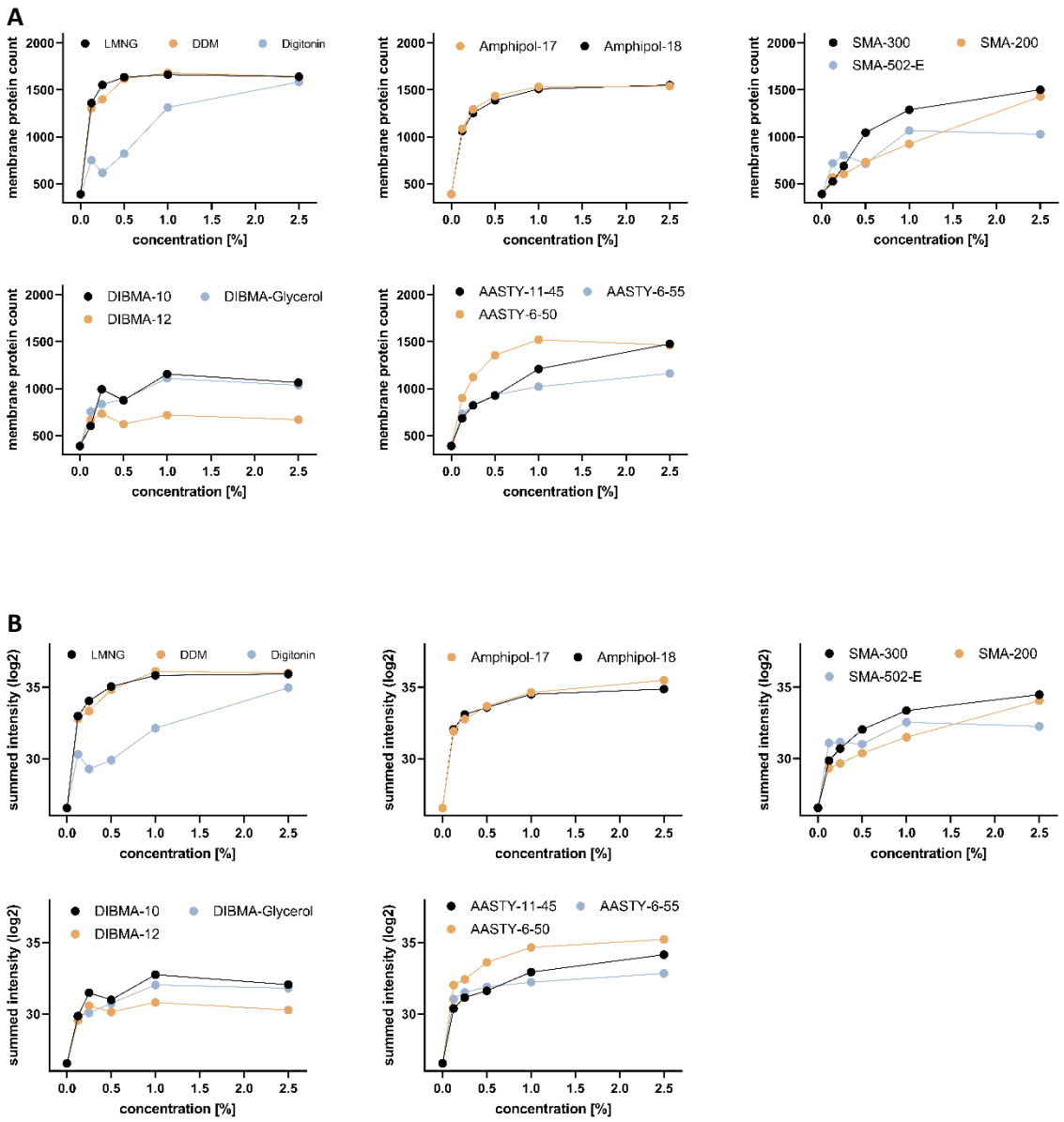

Figure 5. Membrane protein extraction efficiencies of tested solubilization agents. A. Number of unique membrane proteins detected as a function of solubilization agent concentration concentrations (0.125 %, 0.25 %, 0.5 %, 1 % and 2.5 %). **B.** Summed membrane protein intensities as a function of solubilization agent concentration.

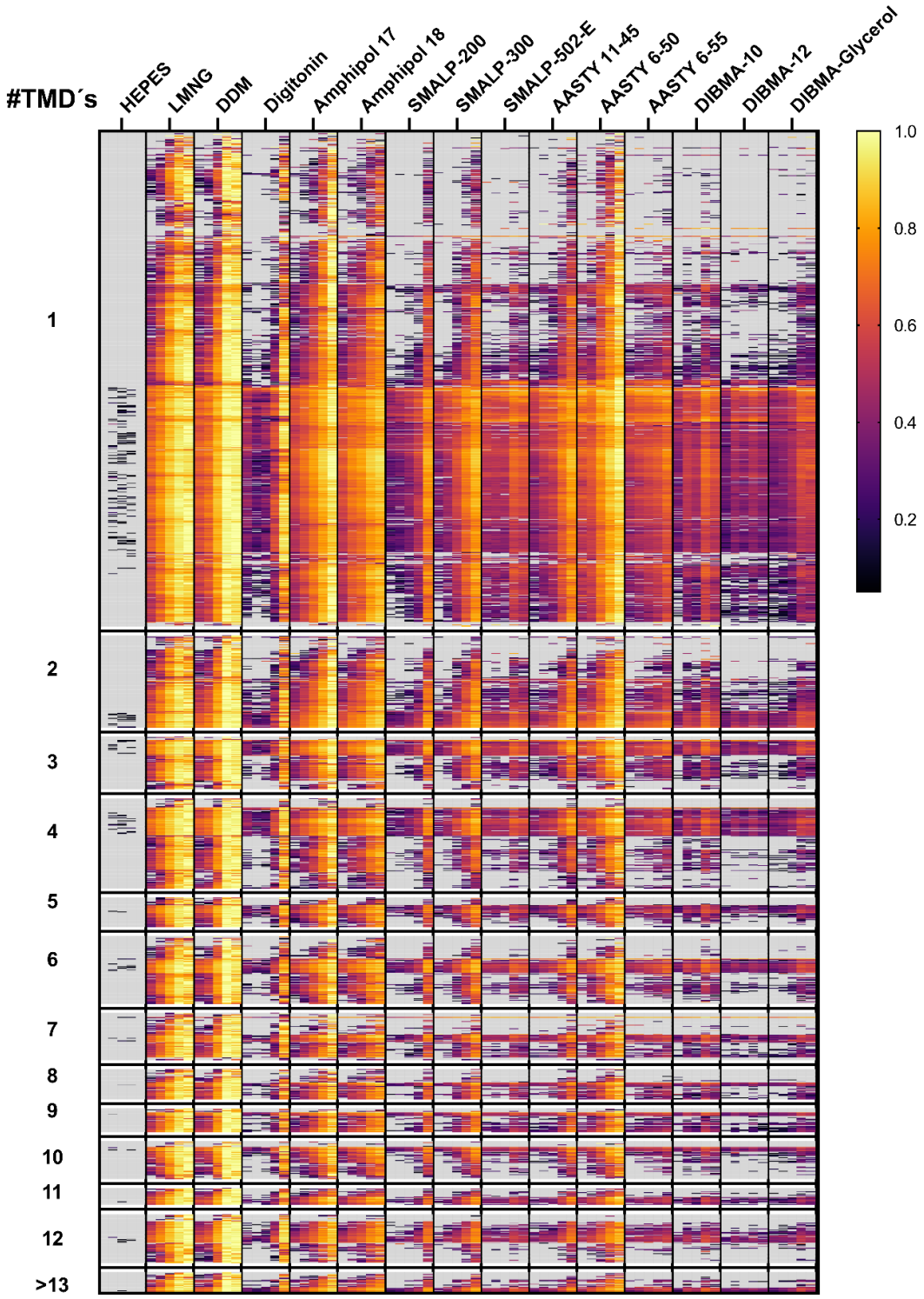

Figure 6. Membrane protein intensities as a function of solubilization agent concentrations. For each solubilization agent, we tested five increasing concentrations (0.125 %, 0.25 %, 0.5 %, 1 % and 2.5 %) which are plotted in columns from left to right. Hepes without any additives was used as control in triplicate. Row in the heat map represent an individual proteins, which were further grouped according to their number transmembrane domains.

625 **Table 1.** Summary of the solubilization agents used in our screening experiments.

Class	Copolymer/detergent	Primary screen	Dilution screen
		2.5%	0.125 – 2.5%
AASTY	AASTY 11-55	yes	No
AASTY	AASTY 6-55	yes	Yes
AASTY	AASTY 11-50	yes	No
AASTY	AASTY 6-50	yes	Yes
AASTY	AASTY 11-45	yes	Yes
Amphipol	Ultrasolute™ Amphipol 18 (CyclAPolC8C0-50)	yes	Yes
Amphipol	Ultrasolute™ Amphipol 17 (CyclAPolC6C2-50)	yes	Yes
DIBMA	DIBMA Glucosamine	yes	No
DIBMA	DIBMA Glycerol	yes	Yes
DIBMA	DIBMA 12	yes	Yes
DIBMA	DIBMA 10	yes	Yes
SMALP	SMALP 502-E	yes	Yes
SMALP	SMALP 300	yes	Yes
SMALP	SMALP 200	yes	Yes
Neutral detergents	Digitonin-A	yes	Yes
Neutral detergents	LMNG	yes	Yes
Neutral detergents	DM	yes	No
Neutral detergents	DDM	yes	Yes
Ionic detergents	RIPA buffer (1 % Nonidet P-40, 0.5 % deoxycholate, 0.1 % SDS)	yes	No
Ionic detergents	SDS	yes, 5%	No
Ionic detergents	SDC	yes	No
Ionic detergents	Fos-12	yes	No
Negative Control	HEPES	yes	Yes

626

627

628 **Supplementary figures**

629 **Supplementary Figure 1 Correspondence between membrane protein mRNA and protein detection**
630 **in Hek293 cells.** RNA transcript counts of membrane protein coding genes were plotted against binned
631 log2 transformed TPM. Transcripts with TPM < 1 were removed. In blue, we show the number of
632 proteins we could detect as a function of their corresponding TPM value obtained from Protein Atlas
633 (See methods).

634

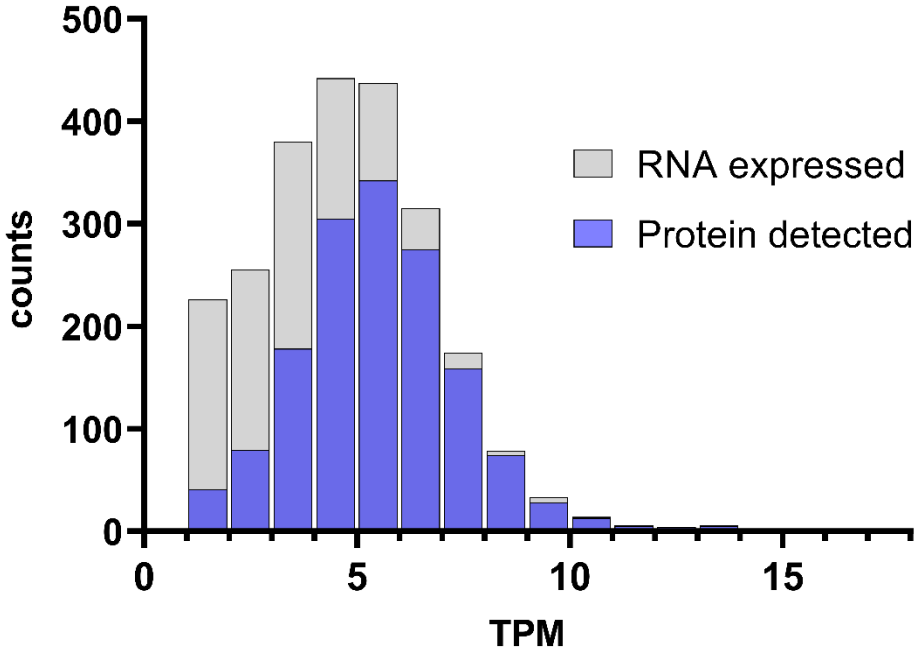

635

636

637

638

639 **Supplementary Table 1. Physicochemical characteristics of all solubilization agents used.**

Copolymer/detergent	Apolar subunit	Polar subunit	Subunit ratio	CMC	Mw	Charge
				% (w/v)	g/mol	
AASTY 11-55	Styrene	Acrylic acid	55:45	n.a.	11,000	Negative
AASTY 6-55	Styrene	Acrylic acid	55:45	n.a.	5,500	Negative
AASTY 11-50	Styrene	Acrylic acid	1:1	n.a.	11,000	Negative
AASTY 6-50	Styrene	Acrylic acid	1:1	n.a.	5,500	Negative
AASTY 11-45	Styrene	Acrylic acid	45:55	n.a.	11,000	Negative
CyclAPolC8C0-50 Ultrasolute Amphipol 18	Cyclooctyl acrylamide	Acrylic acid	1:1	n.a.	7,500	Negative
CyclAPolC6C2-50 Ultrasolute Amphipol 17	2-Cyclohexyl-ethyl acrylamide	Acrylic acid	1:1	n.a.	7,500	Negative
DIBMA Glucosamine	Diisobutylidene	Maleamic acid-glucosamine	1:1	n.a.	14,900	Negative
DIBMA Glycerol	Diisobutylidene	Maleamic acid-3-amino-1,2-propanediol	1:1	n.a.	12,500	Negative
DIBMA 12	Diisobutylidene	Maleic acid	1:1	n.a.	12,000	Negative
DIBMA 10	Diisobutylidene	Maleic acid	1:1	n.a.	10,000	Negative
SMA 502-E	Styrene	Maleic acid monoethyl ester	1.5:1	n.a.	7,000	Negative
SMA 300	Styrene	Maleic acid	3:1	n.a.	10,000	Negative
SMA 200	Styrene	Maleic acid	2:1	n.a.	6,500	Negative
Digitonin-A			n.a	0.2 - 0.3	1,229.31	Neutral
LMNG			n.a	0.001	1,005.19	Neutral
DM			n.a	0.087	482.56	Neutral
DDM			n.a	0.0087	510.62	Neutral
RIPA buffer			n.a	n.a.	n.a.	Some negative (SDS, cholate), some positive (Tris)
SDS			n.a	0.2	288.38	Negative (sulfate)
Fos-12			n.a	0.047	351.5	Neutral (zwitterionic)
HEPES			n.a	n.a.	238.30	Positive (two positive and one negative charges)

640

641

642